

Large Rashba spin splitting of surface resonance bands on semiconductor surface

Shinichiro Hatta and Tetsuya Aruga*

Department of Chemistry, Graduate School of Science, Kyoto University, Kyoto 606-8502, Japan
and JST CREST, Saitama 332-0012, Japan

Yoshiyuki Ohtsubo and Hiroshi Okuyama

Department of Chemistry, Graduate School of Science, Kyoto University, Kyoto 606-8502, Japan
(Received 2 June 2009; revised manuscript received 11 August 2009; published 25 September 2009)

We have found a large spin splitting due to the Rashba spin-orbit interaction on the Bi/Ge(111)- $(\sqrt{3} \times \sqrt{3})R30^\circ$ surface by using angle-resolved photoelectron spectroscopy and first-principles electronic structure calculation. A surface resonance band derived from Bi exhibits the Rashba spin splitting with a large Rashba parameter (α_R) of 1.8 eV Å. The spin-split states have a considerable 6s-6p_z hybridized character, which leads to a strong perpendicular asymmetry of the charge density in close proximity of Bi nuclei. The result suggests that the magnitude of the Rashba splitting on Bi-adsorbed surfaces should depend crucially on the local-bonding geometry of Bi.

DOI: 10.1103/PhysRevB.80.113309

PACS number(s): 73.20.At, 71.70.Ej

The spin splitting of two-dimensional electronic states due to the spin-orbit (SO) interaction arising from structural inversion asymmetry, called Bychkov-Rashba or Rashba effect,¹ is currently a subject of intensive research investigations. The Rashba effect is described by the Rashba Hamiltonian

$$H_R = \alpha_R (\hat{z} \times \mathbf{k}_\parallel) \cdot \boldsymbol{\sigma},$$

for an electron moving in xy plane with a momentum $\hbar \mathbf{k}_\parallel$ under an electric field along z direction $E_z = \partial V / \partial z$, which leads to the quantization of spin $\boldsymbol{\sigma}$ perpendicular to \mathbf{k}_\parallel in xy plane with energy splitting $\Delta_R = 2\alpha_R k_\parallel$. The Rashba parameter α_R serves as a measure of the magnitude of the SO interaction.

The magnitude of the Rashba splitting is governed by *intra*-atomic SO interaction.²⁻⁴ In particular, the surfaces of heavy elements such as ⁷⁹Au,⁵⁻⁷ ⁷⁴W (Refs. 8-10), and ⁸³Bi (Refs. 11-13) exhibit Rashba splitting up to several hundreds of meV. On the other hand, recent observation of even larger Rashba splitting on ⁴⁷Ag surfaces covered with submonolayer Bi^{14,15} suggests that a large Rashba splitting may be “transplanted” to the surfaces of lighter elements, such as ¹⁴Si and ³²Ge, by the adsorption of heavy elements, suggesting a possibility of an application to spintronic semiconductor devices.¹⁶⁻¹⁸

The Rashba parameter is expressed intuitively as

$$\alpha_R \propto \int d\mathbf{r} (\partial V / \partial z) |\psi(\mathbf{r})|^2$$

for a surface state with a wave function $\psi(\mathbf{r})$.¹⁹ This expression directly implies that the major contribution to α_R comes from the close proximity of atomic nuclei, where the bare Coulombic potential due to the nuclei dominates, and that, since the potential gradient is mostly antisymmetric, the asymmetry of $|\psi(\mathbf{r})|^2$ along z direction in the closest proximity of the nuclei governs the magnitude of α_R . Note that any asymmetry of $|\psi(\mathbf{r})|^2$ in xy plane contribute little to α_R , as $\partial V / \partial z$ is negligible.

In this Brief Report, we report a large Rashba splitting of a Bi-induced surface electronic band on the Bi/Ge(111)- $(\sqrt{3} \times \sqrt{3})R30^\circ$ surface [called $(\sqrt{3} \times \sqrt{3})$ hereafter]. Angle-resolved photoelectron spectroscopy (ARPES) shows that a pair of surface-resonance bands are degenerated at \bar{M} but are split at \mathbf{k}_\parallel points away from \bar{M} . A first-principles full-potential calculation reveals that the splitting is due to the Rashba SO interaction. The Rashba parameter is experimentally determined to be 1.8 Å eV, which is larger than that for a surface band on Bi(111). The calculated wave function close to the Bi nucleus indicates that the bonding among Bi and Ge atoms on this surface induces considerable distortion of the wave function, thus, yielding a giant Rashba splitting.

The valence-band ARPES of the $(\sqrt{3} \times \sqrt{3})$ surface was studied by an ARPUS10 electron spectrometer (VG Microtech) with unpolarized He I and Ne I radiation from a rare-gas discharge lamp. All the spectra shown here were obtained from the sample at 110–120 K. The total-energy resolution was 80–100 meV. The work function of the $(\sqrt{3} \times \sqrt{3})$ surface was determined to be 4.51 eV. The Ge(111) substrate (n -type, 0.1–1 Ω cm) was cleaned by repeated cycles of Ar ion sputtering at ~ 700 eV and annealing up to ~ 950 K. Bi was deposited from an alumina or Ta crucible onto the room temperature Ge(111) sample so that coverage slightly exceeds 1 ML, where 1 ML (monolayer) is defined as the atomic density of Ge(111). The subsequent annealing at ~ 700 K for ~ 1 min yielded a sharp and well-contrasted low-energy electron diffraction (LEED) pattern of $(\sqrt{3} \times \sqrt{3})$ as shown in Fig. 1.

The energy bands mapped by ARPES around the second \bar{M} point (\bar{M}_2) of the $(\sqrt{3} \times \sqrt{3})$ surface Brillouin zone (SBZ) along $\bar{\Gamma}-\bar{M}$ are shown in Fig. 2(a). The band map is composed of the grayscale representation of the second derivatives of energy distribution curves (EDCs). It is found that, a pair of bands crosses with each other at \bar{M}_2 at binding energy of ~ 0.85 eV. The upper band disperses upward at k_\parallel points away from \bar{M}_2 , passes a maximum at $k_\parallel = 0.09 \text{ \AA}^{-1}$ from \bar{M}_2

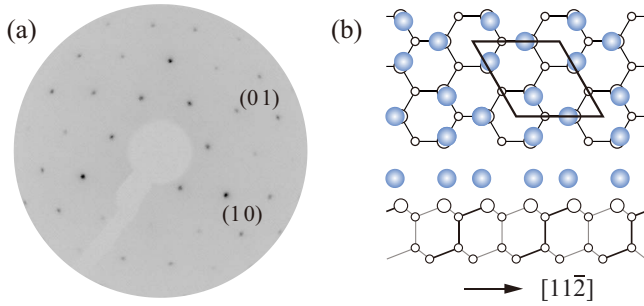


FIG. 1. (Color online) (a) The LEED pattern Bi/Ge(111)- $(\sqrt{3} \times \sqrt{3})R30^\circ$ with 154 eV at 110 K. (b) The top and side views of a milkstool structure. Filled and open circles represent Bi and Ge atoms, respectively.

and disperses downward at larger k_{\parallel} . On the other hand, the lower band disperses monotonously downward from \bar{M}_2 . Note that these bands lie in the projected bulk-band region, for which the upper edge is shown by the solid line. The peak positions determined in EDCs measured with He I and Ne I are summarized in Fig. 2(b). The pair of split bands is observed at the same binding energies for two different photon energies, indicating that the bands are surface resonances.

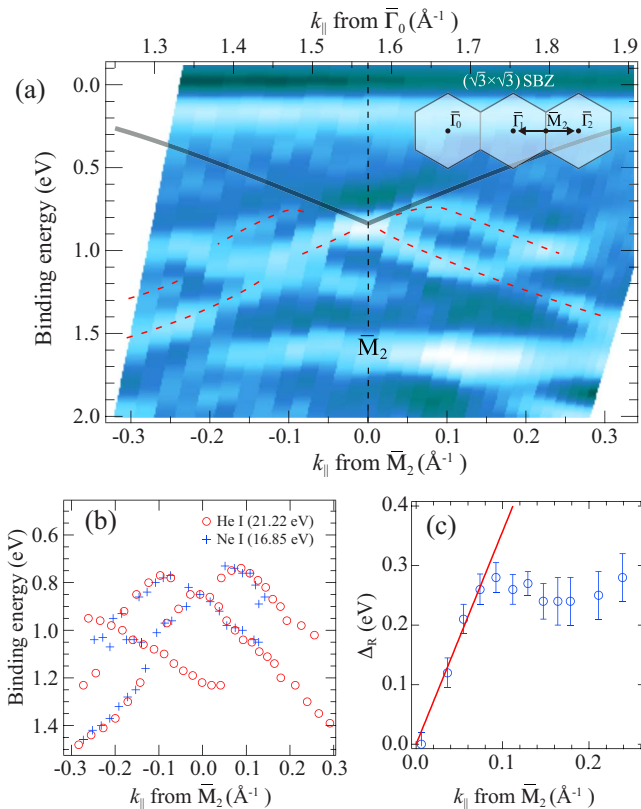


FIG. 2. (Color online) (a) The band structure of the Bi/Ge(111)- $(\sqrt{3} \times \sqrt{3})R30^\circ$ surface around \bar{M} along $\bar{\Gamma}\bar{M}$ measured with $h\nu=21.22$ eV. The solid curves represent the edge of the projected bulk-band region. The inset indicates SBZs and the k_{\parallel} region probed. (b) Peak positions in energy and k_{\parallel} in EDCs measured with $h\nu=21.22$ eV (circles) and $h\nu=16.85$ eV (crosses). (c) Energy splitting plotted as a function of k_{\parallel} from \bar{M}_2 toward $\bar{\Gamma}_2$.

We carried out the structure determination of the $(\sqrt{3} \times \sqrt{3})$ surface by means of the dynamical LEED analysis. We measured diffraction intensity of seven inequivalent beams for a total energy range of 2296 eV. The automated tensor LEED package²⁰ was used to examine eleven models with the p31m symmetry and Bi coverages of 1/3 or 1 ML. We found that the so-called “milkstool” structure with 1 ML Bi,²¹ as shown in Fig. 1(b), best reproduces the experimental data. The Pendry R factor, R_p , for this model was 0.22. The other models yielded $R_p > 0.4$ and were excluded. The center of the Bi trimer resides at the T_4 site (above second-layer Ge) and the lateral positions of three Bi atoms are displaced by 0.55 Å from the neighboring T_1 sites (above first-layer Ge) toward the center. Based on the structure obtained by LEED, we performed the all-electron band calculation with the full-potential linearized augmented plane wave plus local orbitals (APW+lo) method²² and the PBE96 generalized gradient approximation (GGA).²³ The asymmetric slabs of 10 or 23 Ge(111) layers were used with one side covered with the milkstool $(\sqrt{3} \times \sqrt{3})$ -Bi structure and the other side terminated by hydrogen atoms. The vacuum region between neighboring slabs was 20 a.u. thick. The energy cutoff for the plane-wave basis was set at 11.5 Ry and seven k points in the irreducible wedge were sampled. The convergence with respect to the computational parameters was carefully tested. The energetically optimized structural parameters show a quantitative agreement with those optimized by LEED.

Figure 3(a) shows the calculated band structure of the $(\sqrt{3} \times \sqrt{3})$ structure along $\bar{\Gamma}-\bar{M}-\bar{\Gamma}$. The broken lines represent the edge of the projected bulk bands. No occupied surface state is found in the band gap near the Fermi level (E_F). States with significant Bi 6p character are found in the projected bulk-band region, as shown by open and gray circles. These Bi 6p-derived states compose a pair of bands, S_p and S'_p , degenerated at \bar{M} . The radii of open and filled circles represent the contribution of Bi 6p with the spin parallel and antiparallel, respectively, with the $[\bar{2}11]$ direction. The binding energies of the bands S_p and S'_p are in good agreement with the surface resonance bands observed by ARPES, taking into account the fact that the experimental valence-band maximum (VBM) is located ~ 0.2 eV below E_F . The theoretically predicted spin polarization of these states agrees with the Rashba spin splitting. The degeneracy at \bar{M} and their inverted spin polarization with respect to \bar{M} result from the coupling of the time-reversal symmetry and the translational symmetry: $E(\mathbf{G}_{\parallel}/2 + \mathbf{k}_{\parallel}, \uparrow) = E(\mathbf{G}_{\parallel}/2 - \mathbf{k}_{\parallel}, \downarrow)$.

We therefore conclude that the experimentally observed Bi-induced states near \bar{M} are split by the Rashba SO interaction. We plot in Fig. 2(c) the experimental spin splitting as a function of k_{\parallel} from \bar{M} . The splitting increases linearly with k_{\parallel} up to ~ 0.08 Å⁻¹, above which the splitting remains at around ~ 270 meV. The Rashba parameter α_R is evaluated to be 1.8 eV Å, which is to be compared with the value of ~ 0.75 eV Å for the surface bands on Bi(111),¹¹ 3.6 eV Å on Bi/Ag(001),¹⁴ and 3.1 eV Å on Bi/Ag(111).¹⁵

Figure 3 also shows the charge-density plot of S_p at \bar{M} in surface-parallel (111) and surface-normal ($\bar{1}\bar{1}0$) planes, respectively. Mirror planes are along $[11\bar{2}]$ and the equivalent

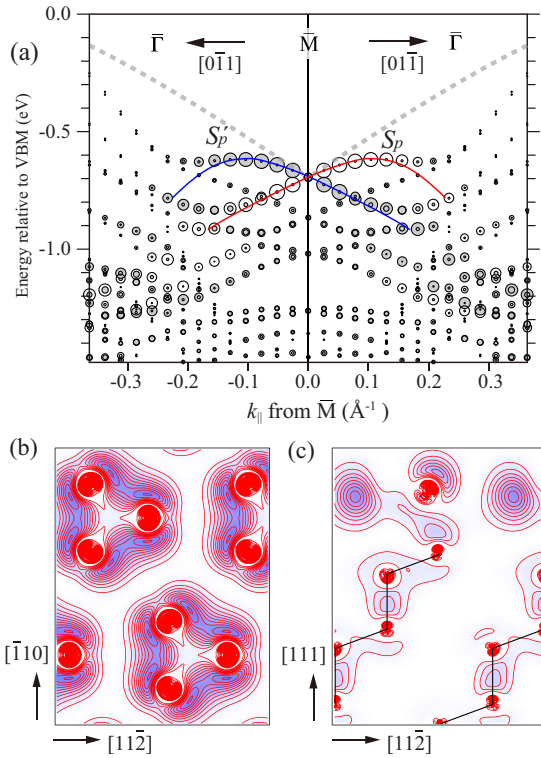


FIG. 3. (Color online) (a) Calculated band structure of the Bi/Ge(111)- $(\sqrt{3} \times \sqrt{3})R30^\circ$ surface at $\bar{\Gamma}$ - \bar{M} - $\bar{\Gamma}$. The radii of open (filled) circles are proportional to the contribution of the Bi $6p$ orbitals with the spin parallel (antiparallel) with the quantization axis $[\bar{2}11]$. Electronic charge-density plots of the S_p state at \bar{M} (b) in a (111) plane and (c) in a $(\bar{1}10)$ plane intersecting the Bi nucleus.

directions. The surface-parallel plot clearly indicates that the state has a character of π -like Bi-Bi bonding orbital derived from $6p_x$ and $6p_y$. The analysis shows that the state also has a contribution of $6p_z$ ($\sim 18\%$ of the contribution of the Bi orbitals) and $6s$ ($\sim 7\%$), which is evident in the surface-normal plot. The relatively small contribution of $6s$ is due to the extra stability of the $6s$ electrons, known as the inert-pair effect of the heavier elements. In our calculation, a surface-state band S_s mainly derived from Bi $6s$ is found at 12–12.5 eV below VBM. The surface-normal plot for S_p shows that the wave function is mostly localized at Bi atoms but penetrates into the Ge layers, indicating the surface resonance character.

The wave function asymmetry along the surface normal with respect to the high- Z Bi nucleus is expected to play an essential role in the giant Rashba spin splitting. Figure 4(a) shows the close-up view of the charge-density plot of S_p at \bar{M} . A slightly asymmetric p -like orbital is tilted by $\sim 35^\circ$ from the surface normal. The tilt is due to the hybridization of $6p_z$ with $6p_x$. The asymmetry of charge density, clearly seen within ~ 0.1 a.u. around the nucleus, indicates that the state has a s character hybridized with the predominant p characters ($s:p_x:p_z=1:1.4:2.6$). The profile of $|\psi|^2$ along the vertical line through the nucleus is shown in Fig. 4(b). The dip is slightly displaced from $z=0$ toward the vacuum, which is due to the contribution of s character. The tilt of the orbital

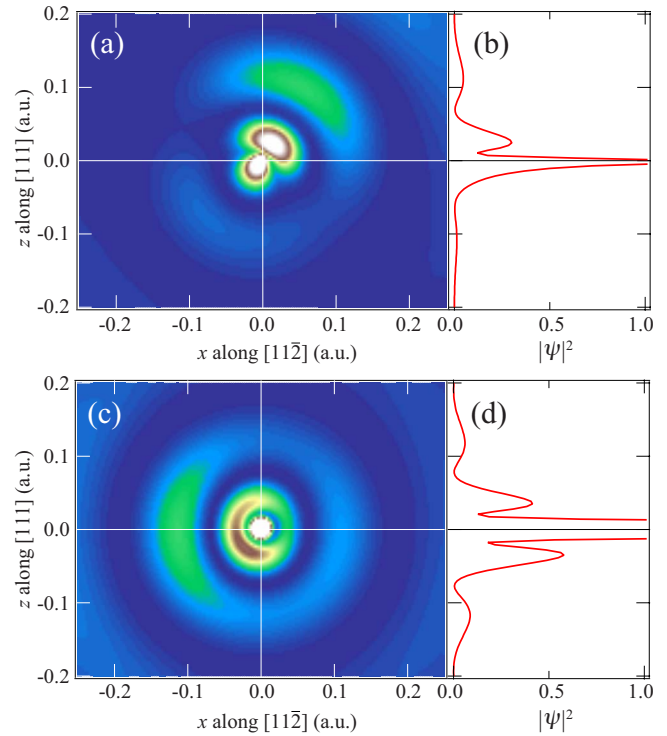


FIG. 4. (Color online) The charge-density plots just around the Bi nucleus of (a) S_p and (c) S_s at \bar{M} , with the Bi nucleus being at the center and the profiles along the vertical line intersecting the Bi nucleus for (b) S_p and (d) S_s at \bar{M} .

results in a large, steep peak close to the nucleus due to the bulk-side lobe and a less prominent peak at 0.03 a.u. from the nucleus due to the vacuum-side lobe in the perpendicular line profile. Since the magnitude of the nuclear potential gradient is proportional to $1/r^2$, r being the distance from the nucleus, the asymmetry at the closest proximity of the nucleus, a dip on the vacuum side and a peak on the bulk side, governs the large α_R value for this state.

The Rashba splitting is also found in the calculated band structure for the surface-state band S_s with the dominant $6s$ character with a small $6p$ (mostly in-plane p_x and p_y) contribution of $\sim 3\%$. The spin splitting is at most 5 meV and α_R is evaluated to be 0.02 eV \AA around \bar{M} . Figure 4(c) shows the charge-density plot of S_s at \bar{M} . While the weak $6p_x$ character is seen, the charge distribution is mostly centrosymmetric. The perpendicular profile shown in Fig. 4(d) indicates that the main peaks within 0.1 a.u. from the nucleus are symmetric, which, when multiplied with antisymmetric $\partial V/\partial z$, gives rise to a negligible contribution to α_R .

The charge density map shown in Fig. 4(a) implies that the perpendicular asymmetry of the wave function should strongly depend on the tilt angle, suggesting the close relation between the local adsorption geometry of Bi and the magnitude of the giant Rashba spin splitting. This may explain the fact that variously sized Rashba spin splitting can appear in different structures with the same pair of the adsorbate and substrate.^{14,15,24–26}

In summary, the large Rashba spin splitting of $\alpha_R = 1.8$ eV \AA is found for the surface-resonance band around

the \bar{M} point on Bi/Ge(111)- $(\sqrt{3} \times \sqrt{3})R30^\circ$. It is shown that the strong potential gradient just around the Bi nucleus contributes to the spin splitting through the vertical asymmetry of the surface-resonance wave function with the hybridized $6s$ and $6p_z$ character. These findings clearly demonstrate that semiconductor surfaces covered with heavy elements are promising as a new field to explore the giant Rashba spin splitting. The study along this line will enable us to study physics such as inequilibrium spin transport at semiconductor surfaces²⁷ and highly efficient spin injection into bulk semiconductors.

Recently, a closely related paper on Bi/Si(111)- $(\sqrt{3} \times \sqrt{3})R30^\circ$ appeared.²⁸ The experimental result by ARPES on the Rashba spin splitting at \bar{M} is very similar to the result presented in this Brief Report.

The authors are indebted to Tamio Oguchi for illuminating discussion and his showing them unpublished results. This work was supported in part by the Global COE Program "Integrated Materials Science" from the Ministry of Education, Culture, Sports, Science, and Technology of Japan (Grant No. B-09).

*aruga@kuchem.kyoto-u.ac.jp

- ¹E. I. Rashba, *Sov. Phys. Solid State* **2**, 1109 (1960); Y. A. Bychkov and E. I. Rashba, *JETP Lett.* **39**, 78 (1984).
- ²R. Winkler, *Spin-Orbit Coupling Effects in Two-Dimensional Electron and Hole Systems* (Springer-Verlag, Berlin, Heidelberg, 2003).
- ³L. Petersen and P. Hedegard, *Surf. Sci.* **459**, 49 (2000).
- ⁴G. Bihlmayer, Yu. M. Koroteev, P. M. Echenique, E. V. Chulkov, and S. Blugel, *Surf. Sci.* **600**, 3888 (2006).
- ⁵S. LaShell, B. A. McDougall, and E. Jensen, *Phys. Rev. Lett.* **77**, 3419 (1996).
- ⁶G. Nicolay, F. Reinert, S. Hüfner, and P. Blaha, *Phys. Rev. B* **65**, 033407 (2001).
- ⁷J. Henk, M. Hoesch, J. Osterwalder, A. Ernst, and P. Bruno, *J. Phys.: Condens. Matter* **16**, 7581 (2004).
- ⁸E. Rotenberg and S. D. Kevan, *Phys. Rev. Lett.* **80**, 2905 (1998).
- ⁹E. Rotenberg, J. W. Chung, and S. D. Kevan, *Phys. Rev. Lett.* **82**, 4066 (1999).
- ¹⁰M. Hochstrasser, J. G. Tobin, E. Rotenberg, and S. D. Kevan, *Phys. Rev. Lett.* **89**, 216802 (2002).
- ¹¹Yu. M. Koroteev, G. Bihlmayer, J. E. Gayone, E. V. Chulkov, S. Blügel, P. M. Echenique, and Ph. Hofmann, *Phys. Rev. Lett.* **93**, 046403 (2004).
- ¹²Ph. Hofmann, *Prog. Surf. Sci.* **81**, 191 (2006).
- ¹³T. Hirahara, T. Nagao, I. Matsuda, G. Bihlmayer, E. V. Chulkov, Yu. M. Koroteev, P. M. Echenique, M. Saito, and S. Hasegawa, *Phys. Rev. Lett.* **97**, 146803 (2006).
- ¹⁴T. Nakagawa, O. Ohgami, Y. Saito, H. Okuyama, M. Nishijima, and T. Aruga, *Phys. Rev. B* **75**, 155409 (2007).
- ¹⁵C. R. Ast, J. Henk, A. Ernst, L. Moreschini, M. C. Falub, D. Pacilé, P. Bruno, K. Kern, and M. Grioni, *Phys. Rev. Lett.* **98**, 186807 (2007).
- ¹⁶S. Datta and B. Das, *Appl. Phys. Lett.* **56**, 665 (1990).
- ¹⁷A. Voskoboynikov, S. S. Liu, C. P. Lee, and O. Tretyak, *J. Appl. Phys.* **87**, 387 (2000).
- ¹⁸T. Koga, J. Nitta, T. Akazaki, and H. Takayanagi, *Phys. Rev. Lett.* **89**, 046801 (2002).
- ¹⁹M. Nagano, A. Kodama, T. Shishidou, and T. Oguchi, *J. Phys.: Condens. Matter* **21**, 064239 (2009).
- ²⁰A. Barbieri and M. A. Van Hove, Symmetrized automated tensor LEED (SATLEED) package (available from M. A. Van Hove, <http://www.ap.cityu.edu.hk/personal-website/Van-Hove.htm>).
- ²¹S. Nakatani, T. Takahashi, Y. Kuwahara, and M. Aono, *Phys. Rev. B* **52**, R8711 (1995).
- ²²P. Blaha, K. Schwarz, G. K. H. Madsen, D. Kvasnicka, and J. Luiz, *WIEN2k, An Augmented Plane Wave+Local Orbitals Program for Calculating Crystal Properties* (Karlheinz Schwarz, Techn. Universität Wien, Wien, Austria, 2001).
- ²³J. P. Perdew, K. Burke, and M. Ernzerhof, *Phys. Rev. Lett.* **77**, 3865 (1996).
- ²⁴S. Hatta, C. Kato, N. Tsuboi, S. Takahashi, H. Okuyama, T. Aruga, A. Harasawa, T. Okuda, and T. Kinoshita, *Phys. Rev. B* **76**, 075427 (2007).
- ²⁵S. Hatta, T. Aruga, C. Kato, S. Takahashi, H. Okuyama, A. Harasawa, T. Okuda, and T. Kinoshita, *Phys. Rev. B* **77**, 245436 (2008).
- ²⁶K. Sakamoto, T. Oda, A. Kimura, K. Miyamoto, M. Tsujikawa, A. Imai, N. Ueno, H. Namatame, M. Taniguchi, P. E. J. Eriksson, and R. I. G. Uhrberg, *Phys. Rev. Lett.* **102**, 096805 (2009).
- ²⁷M.-H. Liu, S.-H. Chen, and C.-R. Chang, *Phys. Rev. B* **78**, 195413 (2008).
- ²⁸I. Gierz, T. Suzuki, E. Frantzeskakis, S. Pons, S. Ostanin, A. Ernst, J. Henk, M. Grioni, K. Kern, and C. R. Ast, *Phys. Rev. Lett.* **103**, 046803 (2009).